CENTER FOR
MACHINE PERCEPTION

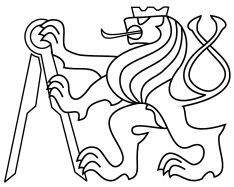

CZECH TECHNICAL
UNIVERSITY IN PRAGUE

BACHELOR THESIS

Robust Focal Length Computation

Oleh Rybkin

rybkiole@fel.cvut.cz

May 18, 2017

Available at
WritethefullURLofthepaperhere,ifavailableintheelectronicform.

Thesis Advisor: Ing. Tomáš Pajdla, PhD.

Acknowledge grants here. Use centering if the text is too short.

Center for Machine Perception, Department of Cybernetics
Faculty of Electrical Engineering, Czech Technical University
Technická 2, 166 27 Prague 6, Czech Republic
fax +420 2 2435 7385, phone +420 2 2435 7637, www: http://cmp.felk.cvut.cz

Robust Focal Length Computation

Oleh Rybkin

May 18, 2017

Text of acknowledgements...

Author's declaration

I declare that I have work out the presented thesis independently and that I have listed all information sources used in accordance with the Methodical Guidelines about Maintaining Ethical Principles for Writing Academic Theses.

Prohlášení autora práce

Prohlašuji, že jsem předloženou práci vypracoval samostatně a že jsem uvedl veškeré použité informační zdroje v souladu s Metodickým pokynem o dodržování etických principů při přípravě vysokoškolských závěrečných prací.

V Praze dne ....

Podpis autora práce

Text of abstract...

Contents

List of Symbols and Abbreviations

x	Scalar value.
$\mathbf{x}$	Column vector.
$\mathtt{X}$	Matrix.
X	Set.
$\mathbb{C}$	Complex numbers field.
$\mathbb{R}$	Real numbers field.
$\mathrm{K}[x_1, x_2, x_3, \ldots, x_n]$	Polynomial ring in variables $x_1, x_2, x_3, \ldots, x_n$ over the field K.
$\mathbb{R}^n$	Linear space of dimension n over real numbers.
$\mathbb{P}^{n-1}$	Projective space of dimension $n-1$ over real numbers.
$\mathbf{x} \otimes \mathbf{y}$	Kronecker (outer) product of vectors $\mathbf{x}$,$\mathbf{y}$.
$[x]_\times$	Cross product matrix, i.e. a matrix multiplication by which represents a cross product with vector x.
$\det \mathtt{X}$	Determinant of the matrix $\mathtt{X}$.
$\operatorname{diag} \mathbf{x}$	Diagonal matrix that have elements of $\mathbf{x}$ at its diagonal.
$\operatorname{vec} \mathtt{X}$	Vector produced by stacking columns of the matrix $\mathtt{X}$.
$\mathtt{I}$	Identity matrix.
$\mathtt{0}_{x,y}$	Zero matrix from $\mathbb{R}^{x \times y}$.
$\mathcal{N}(\mu, \sigma^2$	Gauss distribution with mean μ and standard deviation σ.

List of Figures

1 Introduction

We analyze the problem of computing epipolar geometry of two partially calibrated cameras, where only focal lengths are unknown.

Estimating epipolar geometry with unknown focal lengths is an important issue in practical problems. In laboratory environment it is possible to calibrate the camera beforehand using established procedures [**?**]. TP: When taking images in the wild, however, it is often impractical or impossible to use these procedures. It is desirable to have an automated procedure to estimate camera calibration from images themselves.

The usual way [**?**, **?**, **?**] to estimate camera external and internal parameters is to extract points of interests [2, 18] with tentative correspondences, and use RANSAC [**?**] method for joint estimation of correspondence inlier pairs and camera parameters. In RANSAC, a procedure to compute camera parameters from a (preferably small) number of points is needed. These procedures, that essentially are used as black box in RANSAC, are called minimal problems because it is desirable to find a procedure that would use the theoretical minimum number of points.

The basic procedure to compute the focal lengths and epipolar geometry given correspondences consists of two steps: finding a Fundamental matrix and decomposing the matrix into Calibration matrices and Essential matrix. For the first task, the minimal number of correspondences needed is 7. Hartley and Zisserman [8] describe an algorithm for this which uses 7 correspondences as well as the singularity condition. The algorithm gives three different estimations of the matrix, i.e. one correct and two false ones. Hartley [10] also summarizes an algorithm by Longuet-Higgins [17] which uses 8 correspondences instead. Bougnoux [3] gives a concise formula to compute focal length from the fundamental matrix, if principal point position is known. TP: All calibration information except for the focal lengths mut be know, i.e. the principal point, the skew, the ratio of the pixel dimensions.

The procedure suffers from a number of known failure cases:

- It is not possible to determine a Fundamental matrix if the correspondences are in singular position.
- The computed Fundamental matrix may have intersecting (or parallel) optical axes. TP: IT is not the property of the fundamental matrix but of the camera arrangement. Reformulate.In that case it is impossible to determine the focal lengths.
- All computed Fundamental matrices may have rank 1 or be complex.
- A computed focal length may be complex.
- There may be no such computed camera configuration where most points in 3D space lie in front of the cameras.

Because of these deficiencies, the commonly held view is that the algebraic approach of using 7pt algorithm and Bougnoux formula is not robust, and sometimes fails entirely, unable to find any valid solution. Hartley [9] argues that in many practical cases this approach cannot be used and other methods [9, 22, 13] were proposed to solve this problem.

We analyze the procedure TP: of what? and different degeneracies to show that slight modifications of the procedure allow to alleviate a number of the problems. We show that the algorithm can perform reasonably well in practice.

2 Basic notions

2.1 Camera geometry

The book [8] describes camera geometry, the main topic of this thesis, in chapter 6. All needed preliminaries are also well described in chapters 1-5 of the book. In the next two sections we very briefly summarize and recapitulate the topic. We follow the notation of [8].

2.1.1 Single camera geometry

The most convenient way of representing points in 3D or 2D space while dealing with camera geometry is using corresponding projective spaces.

Definition 2.1.1. Given a linear vector space $\mathbb{R}^n$, a *projective space* $\mathbb{P}^{n-1}$ could be defined as a factorization of the linear space by a relation $\sim$:

$$\mathbf{x}_1 \sim \mathbf{x}_2 \iff (\exists \lambda \in \mathbb{R}\backslash\{0\}\ \mathbf{x_1} = \lambda \mathbf{x_2}).$$

Zero point is also excluded from projective space.

A point $\mathbf{X}_i = \begin{bmatrix} x & y & z \end{bmatrix}^{\mathrm{T}}$ from 3D linear space $\mathbb{R}^3$ can be though of as a point $\mathbf{X'} = \begin{bmatrix} x & y & z & 1 \end{bmatrix}^{\mathrm{T}}$ from 3D projective space $\mathbb{P}^3$. Similarly, a point $\mathbf{X'} = \begin{bmatrix} x & y & z & f \end{bmatrix}^{\mathrm{T}}$ can be converted back to the point $\mathbf{X} = \begin{bmatrix} \frac{x}{f} & \frac{y}{f} & \frac{z}{f} \end{bmatrix}^{\mathrm{T}}$ unless f is zero. Because of this possible conversion we will frequently refer to the same geometrical point as belonging to projective space $\mathbb{P}^n TP : -1$ as well as linear space $\mathbb{R}^n$ simultaneously.

Definition 2.1.2. A *projective line* is a line of points in projective space $\mathbb{P}^n$. Conveniently, it can be also expressed by a vector from the space $\mathbb{P}^n TP : +1$. For example, a line in projective plane $ax + by + fc = 0$, which corresponds to the line $ax + by + c = 0$ in real plane, can be written as a vector $\mathtt{l} = \begin{bmatrix} a & b & c \end{bmatrix}^{\mathrm{T}}$.

The figure 2.1 shows an essential concept of projecting points from world (3D) space to image (2D) space. This projection can be described as a linear operation in corresponding projective spaces.

The projection operator is given by camera parameters, which can be divided in two groups - extrinsic and intrinsic parameters. We next define essential intrinsic parameters.

Definition 2.1.3. *The principal axis*, also *optical axis*, is the line passing through camera center and perpendicular to the image plane.

Definition 2.1.4. *The principal point* $\mathbf{p} = \begin{bmatrix} p_x & p_y & 1 \end{bmatrix}^{\mathrm{T}}$ is the point lying at the intersection of image plane and principal axis.

Definition 2.1.5. *The focal length* f is the distance from the camera center to the principal point.

Camera intrinsic parameters are can be formed into camera calibration matrix.

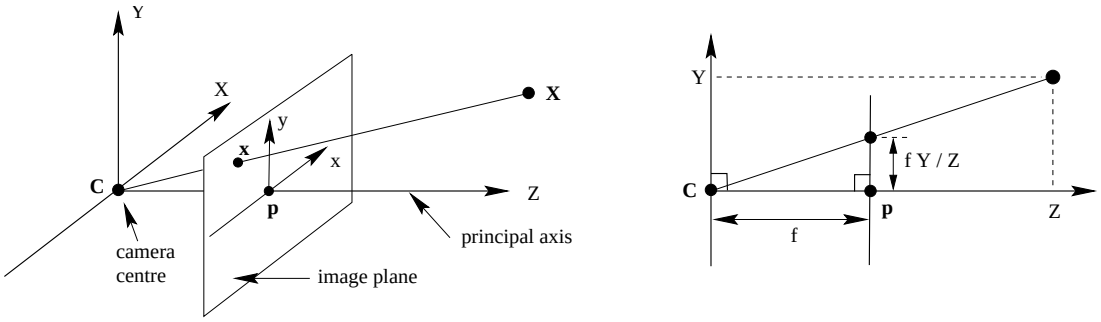

Figure 2.1 Camera model. Courtesy [8]

Definition 2.1.6. *A calibration matrix*[1] $\mathtt{K}$ is a matrix of the form

$$\mathtt{K} = \begin{bmatrix} f & 0 & p_x \\ 0 & f & p_y \\ 0 & 0 & 1 \end{bmatrix}.$$

The matrix is defined up to scaling. TP: this is not clear. The matrix is not really defined up to scale when you write it with $K_{33} = 1$.

If we assume that the camera center is the world space zero point, principal axis coincide with Z axis, and image space axes x, y are aligned with world space axes X, Y (true for the figure 2.1), we can project 3D points with only camera intrinsics. The projection from $\mathbb{R}^3$ to $\mathbb{P}^2$ image plane is given by $\mathbf{x}_i = \mathtt{K}\mathbf{X}_i$.

Extrinsic parameters of a camera i are described by a rotation matrix in the world space $\mathtt{R}_i$ describing camera orientation and the camera center point $\mathbf{C}_i$ in the world space. Given extrinsic and intrinsic parameters, we can construct the full projection matrix.

Definition 2.1.7. The camera *projection matrix* $\mathtt{P}_i$ can be constructed from camera parameters and projects points $\mathbf{X}_i$ from world space $\mathbb{P}^3$ to the image plane $\mathbb{P}^2$:

$$\mathbf{x}_i = \mathtt{P}\mathbf{X}_i = \mathtt{KR}[\mathtt{I}|-\mathbf{C}]\mathbf{X}_i$$

.

2.1.2 Epipolar geometry

Epipolar geometry, the main topic TP: Not true. The main topic is robust comptution of f. of this thesis, is a geometry of two cameras seeing the same 3D object.

This section is described in depth in chapter 9 of [8]. As a slight deviation from the notation of Hartley and Zisserman, cameras and respective image points are indexed with numbers, e.g., $\mathbf{x}_1$, $\mathbf{x}_2$ and not $\mathbf{x}$, $\mathbf{x}'$ respectively. We make this change so that an arbitrary number of cameras could be accounted for.

Extrinsic parameters of a camera pair can be concisely given by the translation vector between camera centers $\mathbf{t} = \mathbf{C}_1 - \mathbf{C}_2$ and the rotation matrix between cameras' coordinate systems $\mathtt{R} = \mathtt{R}_2\,\mathtt{R}_1^T$. If $\mathtt{R}, \mathbf{t}$ are known, extrinsics $\mathtt{R}_1, \mathtt{R}_2, \mathbf{C}_1, \mathbf{C}_2$ are defined up to a projective transformation.

Geometry of two cameras and a point is usually described in terms of epipoles, the key concept of epipolar geometry.

[1] Throughout this work we assume unity aspect ratio and zero skew.

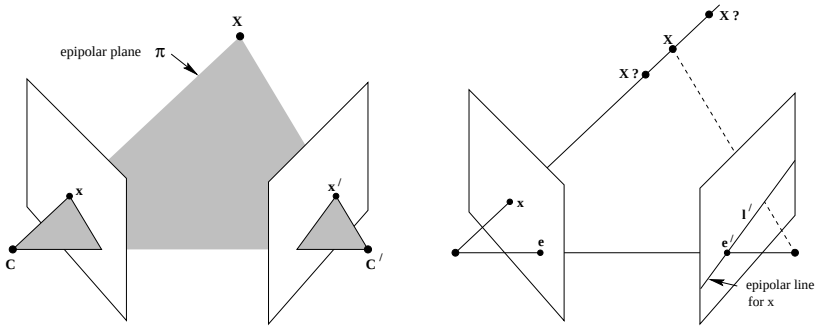

Figure 2.2 Camera pair. Courtesy [8]

Definition 2.1.8. *The epipole* $\mathbf{e}_i$ is the point in image plane that lies at the line joining camera centers. Equivalently, it is the point to which the center of another camera projects.

Definition 2.1.9. *An epipolar line* $\mathbf{l}$ is a line in image plane on which the epipole of that plane lies.

Definition 2.1.10. *An epipolar plane* π is a plane in the world space which contains the line joining camera centers. The plane is associated with two epipolar lines that it also contains.

The information about camera epipolar geometry can be described by a single matrix as defined next. If interested, see extended discussion and proofs in [8].

Definition 2.1.11. *An Essential matrix* $\mathtt{E}$ is a matrix of the form $\mathtt{E} = \mathtt{R}[\mathbf{t}]_\times$. The essential matrix is defined up to overall scaling.

As can be seen from its construction, an essential matrix can only be of rank 2. A weaker version of this constraint can be stated as the rank constraint:

$$\det \mathtt{E} = 0. \tag{2.1}$$

The two non-zero singular values of an essential matrix are equal. This constraint can be stated as the next matrix equation (also called the trace constraint):

$$2\mathtt{E}\mathtt{E}^{\mathrm{T}}\mathtt{E} - \operatorname{trace}(\mathtt{E}\mathtt{E}^{\mathrm{T}})\mathtt{E} = 0. \tag{2.2}$$

The equations 2.1 and 2.2 together are named Demazure polynomials [19].

Essential matrix does not capture intrinsic camera parameters. To that end, we use the fundamental matrix.

Definition 2.1.12. *The Fundamental matrix* $\mathtt{F}$ corresponding to an Essential matrix $\mathtt{E}$ is given by

$$\mathtt{F} = \mathtt{K}_2^{-\mathrm{T}}\mathtt{E}\mathtt{K}_1^{-1}. \tag{2.3}$$

The fundamental matrix is, like the essential matrix, defined up to overall scaling.

The fundamental matrix of a camera pair defines a specific mapping from points in one image to epipolar lines in another image. Suppose that given an image point $\mathbf{x}_1 \in \mathbb{P}^3$ and two cameras $\mathtt{P}_1$, $\mathtt{P}_2$, the line $\mathbf{C}_1\mathbf{x}_1$ in world space is projected by the second

camera to the line $\mathbf{l}_2 \in \mathbb{P}^3$ in the second camera image space. Then we can obtain $\mathbf{l}_2$ by $\mathbf{l}_2 = \mathtt{F}\mathbf{x}_1$

For each corresponding image points pair $\mathbf{x}_1, \mathbf{x}_2$, the Fundamental matrix satisfies the so-called Epipolar constraint:

$$\mathbf{x}_2^{\mathrm{T}}\mathtt{F}\mathbf{x}_1 = 0. \tag{2.4}$$

As with essential matrices, a fundamental matrix can only be of rank 2. On the other hand, every matrix of rank 2 is a fundamental matrix [**?**]. A fundamental matrix also satisfies the rank constraint

$$\det \mathtt{F} = 0. \tag{2.5}$$

A version of trace constraint on fundamental matrix can be formulated by substituting equation 2.3 into equation 2.2.

2.2 Computing focal lengths from point correspondences

Given a set of points in one image X_1 and a set of points in another image X_2 that correspond to the same points X in world space, it is possible in some cases to determine the positions of points X and camera intrinsic and extrinsic parameters. This section guides the reader through the process.

Note, that in this part we assume that the point correspondences are given to us by a black box algorithm. In fact, many algorithms and modifications to them were developed to this end, the most notable being the RANSAC family of algorithms [6].

2.2.1 Fundamental matrix computation

First, we need to estimate TP: the fundamental matrix $\mathtt{F}$ of a camera pair. In fact, all the information we need is contained in this matrix. Various algorithms exist that can compute the matrix $\mathtt{F}$ from point correspondences. We present two methods that are, to our best knowledge, used the most. They are relatively simple and can be implemented efficiently.

The algorithms which we will present belong to a family of so-called algebraic solvers, which work by way of constructing a set of constraints on the matrix $\mathtt{F}$ given the correspondences, and then solving the constraints in an algebraically precise way, also giving all possible solutions. If the constraints are represented by polynomial equations TP: delete (which, as we will see, they are), the techniques of algebraic geometry can be used to solve these constraints.

We first define the 7pt algorithm. The algorithm uses (at least) 7 epipolar constraints 2.4 and the rank constraint 2.5. This gives us 8 constraints on a 3×3 matrix. Note, however, that all of the constraints are homogeneous polynomials, and thus the solution to the system will be a finite number[2] of linear one-dimensional spaces of matrices. As a Fundamental matrix is defined up to scaling, this corresponds to a finite number of Fundamental matrices. Moreover, the number of matrices can be expected to be no more than 3, because of the constraints used[3].

The algorithm uses SVD procedure which serves as implicit optimization of epipolar constraints. In case that precisely 7 epipolar constraints are given, SVD can be replaced with Gauss-Jordan elimination, and the $\mathbf{f}_1$, $\mathbf{f}_2$ vectors will be a basis of right null space

[2] We suppose that the constraints are algebraically independent. Equivalently, at least 7 of the correspondence point pairs are in general position.

[3] This number is calculated as the product of degrees of the polynomials $= 3 \cdot 1^7$

of the matrix $\mathtt{B}$. Equivalently, the matrices $\mathtt{F}_1$, $\mathtt{F}_2$ will be a basis of a space of matrices that satisfy the 7 epipolar constraints.

Data: list of $n \geq 7$ right image points $\mathbf{x}_{1,i}$, list of the corresponding left image points $\mathbf{x}_{2,i}$
Result: Fundamental matrix $\mathtt{F}$
begin
  Populate matrix $\mathtt{B} \in \mathbb{R}^{n\times 9}$ with columns $\mathbf{b}_i$: $\mathbf{b}_i \leftarrow \mathrm{vec}(\mathbf{x}_{2,i} \otimes \mathbf{x}_{1,i})$;
  TP: udefined $\otimes$
  Take the right singular vectors $\mathbf{f}_1, \mathbf{f}_2$ corresponding to the two smaller TP: smallest singular values and transform them back to matrices $\mathtt{F}_1, \mathtt{F}_2 \in \mathbb{R}^{3\times 3}$;
  if $\det(\mathtt{F}_2) = 0$ **then**
    return $\mathtt{F}_2$;
  else
    Solve the 3rd degree polynomial in x: $\det(x\mathtt{F}_1 + \mathtt{F}_2) = 0$, and choose the real roots x_i.;
    return $x_i\mathtt{F}_1 + \mathtt{F}_2$;
  end
end

Algorithm 1: 7pt

Note, that we call this algorithm 7pt because the minimal number of correspondences it needs is 7. Nevertheless, any number bigger than 7 can also be used.

The second algorithm doesn't use the rank constraint 2.5. Therefore, generically we expect the result to be a matrix of rank 3 and not a valid Fundamental matrix. The matrix, however, 'better' satisfies the epipolar constraints 2.4. We will compare the performance of that algorithm to 7pt in later parts of the work. Note that this algorithm gives precisely one real solution.

Data: list of $n \geq 8$ right image points $\mathbf{x}_{1,i}$, list of the corresponding left image points $\mathbf{x}_{2,i}$
Result: Fundamental matrix $\mathtt{F}$
begin
  Populate matrix $\mathtt{B} \in \mathbb{R}^{n\times 9}$ with columns $\mathbf{b}_i$: $\mathbf{b}_i \leftarrow \mathrm{vec}(\mathbf{x}_{2,i} \otimes \mathbf{x}_{1,i})$;
  Take the right singular vector $\mathbf{f}$ corresponding to the smaller singular value and transform it back to matrix $\mathtt{F} \in \mathbb{R}^{3\times 3}$;
  return $\mathtt{F}$;
end

Algorithm 2: 8pt

Note, that we call this algorithm 8pt because the minimal number of correspondences it needs is 8. Nevertheless, any number bigger than 8 can also be used.

2.2.2 Essential matrix computation

If the two focal lengths and the principal points are known TP: all other calibration has to be known too, we can estimate essential matrix $\mathtt{E}$ instead of $\mathtt{F}$. This can be done by transforming points so that effects of intrinsic camera parameters are removed:

$$\tilde{\mathbf{x}}_i = \mathtt{K}_i^{-1}\mathbf{x}_i.$$

Then the epipolar constraint 2.4 is satisfied by the essential matrix with respect to the transformed points:

$$\tilde{\mathbf{x}}_2^{\mathrm{T}}\mathtt{E}\tilde{\mathbf{x}}_1 = \mathbf{x}_2^{\mathrm{T}}\mathtt{K}_2^{-\mathrm{T}}\mathtt{E}\mathtt{K}_1^{-1}\mathbf{x}_1 = \mathbf{x}_2^{\mathrm{T}}\mathtt{F}\mathbf{x}_1 = 0.$$

The algebraic solver for essential matrix uses the rank constraint 2.1, the trace constraint 2.2, and needs 5 point correspondences. Note that the trace constraint is a matrix equation, and therefore actually stands as more than one constraint, which explains why counting degrees of freedom seemingly fails in this case.

The construction of the solver is considerably more involved than the previous algorithms, therefore we will only refer to the papers that fully describe it.

Stewenius et al. [20] TP: thre were othe ralgortihms presented before, e.g. by Nister, ... show in detail how to construct an algebraic solver for this problem. The paper is the first one to clearly solve the problem and makes extensive use of theory of algebraic geometry [5][4]. It is very instructing to read through the construction of this solver.

We will, however, use another solver, described by Kukelova et al. in [16]. The code can be found online at "http://cmp.felk.cvut.cz/mini/"[4]. This solver, contrary to one of Stewenius et al., makes it possible to use an arbitrary number of correspondences, which we will take advantage of. We will refer to this solver as *5pt solver*.

For those interested, Kukelova et al. give an algorithm (with source code) that automatically creates solvers for algebraic problems [15].

2.2.3 Focal lengths computation

Bougnoux [3] gives a concise formula to compute focal length from the fundamental matrix, if principal point position is known. In the next two formulae the matrix $\mathtt{I}_2$ is defined as $\mathtt{I}_2 = \mathrm{diag}(1, 1, 0)$, and $\mathbf{e}_1, \mathbf{e}_2$ are the epipoles of first and second image correspondingly.

$$f_1^2 = -\frac{\mathbf{p}_2^{\mathrm{T}} \left[\mathbf{e}_2\right]_\times \mathtt{I}_2\mathtt{F}\mathbf{p}_1\mathbf{p}_1^{\mathrm{T}}\mathtt{F}^{\mathrm{T}}\mathbf{p}_2}{\mathbf{p}_2^{\mathrm{T}} \left[\mathbf{e}_2\right]_\times \mathtt{I}_2\mathtt{F}^{\mathrm{T}}\mathtt{I}_2\mathtt{F}\mathbf{p}_2} \tag{2.6}$$

$$f_2^2 = -\frac{\mathbf{p}_1^{\mathrm{T}} \left[\mathbf{e}_1\right]_\times \mathtt{I}_2\mathtt{F}^{\mathrm{T}}\mathbf{p}_2\mathbf{p}_2^{\mathrm{T}}\mathtt{F}\mathbf{p}_1}{\mathbf{p}_1^{\mathrm{T}} \left[\mathbf{e}_1\right]_\times \mathtt{I}_2\mathtt{F}\mathtt{I}_2\mathtt{F}^{\mathrm{T}}\mathbf{p}_1} \tag{2.7}$$

The second equation may be derived from the first by changing indices and transposing the $\mathtt{F}$ matrix.

Note that it is not possible to find a focal length unless the principal point is known. As these formulae show, TP: delet generically the focal lengths are different for different principal point positions.

2.2.4 Failure cases

We consider the failure cases that may occur while estimating focal length using 7pt algorithm and the Bougnoux formula.

Degeneracies

The first possible degeneracy is that the 7 epipolar constraints 2.4 are *linearly dependent*. This means that the system is underconstrained and there will be generically an infinite number of solutions. A configuration of 7 correspondences which lead to such a system is said to be in singular position.

Agarwal et al. TP: write "al.\" in the LaTeX source code to avoid extra space after "."], in a thorough study [1], consider from the viewpoint of algebraic geometry TP: reorder the words to get a valid English sentence a degeneration when neither of 3 solutions that 7pt gives are actually valid Fundamental matrices. It is shown in the

[4]Enter 'Polynomial eigenvalue solutions to minimal problems in computer vision' in the search field.

paper that meeting the rank constraint is not enough for a matrix to be a fundamental matrix, as it needs to be of rank precisely 2. There may be a degeneracy when the matrix *is of rank 1*[5]. However, the constraint "is not of rank 1" cannot be expressed algebraically in an easy way and doesn't reduce the number of degrees of freedom of F, as it only affects an infinitely small percen TP: fraction of matrices. The preferable way of dealing with this degeneracy is thus to select only valid subset of 3 solutions given by 7pt TP: algorithm.

Another degeneracy may occur when the computed Fundamental matrix TP: This is a property of the cameras arrangement not the fundamental matrix has *intersecting (or parallel) optical axes*. In that case it is impossible to determine the focal lengths [12]. We now formulate a concise condition which describeTP: s when this can happen.

Lemma 2.2.1. *Optical axes of cameras* $\mathtt{P}_1, \mathtt{P}_2$ *as lines in projective* $\mathbb{P}^3$ *space intersect*[6] *if and only if the principal points TP:* $\mathbf{p}_1$, $\mathbf{p}_2$ *satisfy the epipolar constraint*

$$\mathbf{p}_2^T \mathtt{F} \mathbf{p}_1 = 0.$$

Moreover, if the principal points are zero points $\mathbf{p}_1 = \mathbf{p}_2 = \begin{bmatrix} 0 & 0 & 1 \end{bmatrix}^T$, *the optical axes intersect if and only if the rightmost lowest element of the corresponding fundamental matrix* $\mathtt{F}$ *is zero*

$$\mathtt{F}_{3,3} = 0$$

.

Proof. The first part. If optical axes intersect, the point at their intersection is projected to images' principal points. Thus, principal points form a correspondence and must satisfy the epipolar constraint. Conversely, if the principal points satisfy the epipolar constraint, they must lie in an epipolar plane (see figure 2.2). The optical axes are then also lying in the epipolar plane, and each two projective lines in a plane intersect.

The second part. Consider the following:

$$\mathbf{p}_2^{\mathrm{T}} \mathtt{F} \mathbf{p}_1 = \begin{bmatrix} 0 & 0 & 1 \end{bmatrix} \begin{bmatrix} \mathtt{F}_{1,1} & \mathtt{F}_{1,2} & \mathtt{F}_{1,3} \\ \mathtt{F}_{2,1} & \mathtt{F}_{2,2} & \mathtt{F}_{2,3} \\ \mathtt{F}_{3,1} & \mathtt{F}_{3,2} & \mathtt{F}_{3,3} \end{bmatrix} \begin{bmatrix} 0 \\ 0 \\ 1 \end{bmatrix} = \begin{bmatrix} 0 & 0 & 1 \end{bmatrix} \begin{bmatrix} \mathtt{F}_{1,3} \\ \mathtt{F}_{2,3} \\ \mathtt{F}_{3,3} \end{bmatrix} = \mathtt{F}_{3,3}$$

□

Invalid solutions

There are also cases when the matrix and the focal lengths can be computed but don't correspond to any real camera configuration.

Some solutions that may need to be filtered out are *complex* $\mathtt{F}$ *matrices*. As in the 7pt algorithm we are solving a 3rd degree polynomial, we may end up with 2 complex and one real solution TP: reorder words to make it a valid E sentence. This might be a problem if the real solution $\mathtt{F}$ is a matrix on rank 1, and thus we don't have any valid estimate.

Hartley in a work [9] shows that the focal lengths computed TP: delete: from the matrix may be TP: all *complex*, which again leads to impossible camera configuration. This happens because the focal length enter the Bougnoux equation 2.6 only squared,

[5] We suppose that algorithm does not return zero solution $\mathtt{F} = 0_{3,3}$. There indeed exists a formulation in which such solution naturally does not come up.

[6] In projective space we say that two parallel lines intersect at a point at infinity.

so a negative estimation of f^2 leads to a purely imaginary focal length and can occur even when all the coefficients are real. Hartley argues that this is unacceptable and addresses the problem by developing a new algorithm to find a matrix which will have a valid focal length. We will address the degeneracy in this work later, and provide a clear and concise way to correct such a matrix.

Another problem is described in conjunction with the notion of *cheirality* in [11]. In the projective camera model, we allow the points from behind the camera to be projected to image plane. This introduces an ambiguity when decomposing the essential matrix into rotation and translation. Four different camera pairs can be TP: constructed imagined TP: , never comes before "that" in this way. This is a slavism. that will have the same essential matrix, corresponding to two possible orientations of each camera, one that has points in front of it and one that has points behind.

Normally, we are able to pick the right reconstruction by selecting the camera pair such that cameras have points in front of them in world space. However, with presence of TP: large noise it can happen that no such camera pair will exist. Usually the configuration that has the points in front of it is chosen TP: delete , but this strategy can produce a wrong configuration.

2.3 Algebraic Geometry

This section serves as a brief introduction of the topic of algebraic geometry. We follow the notation of Cox et al. from [5][4]. We refer an interested reader to these books.

First we define the key algebraic object of the algebraic geometry.

Definition 2.3.1. Given a polynomial ring $\mathbb{C}[x_1, x_2, \ldots, x_n]$, *an ideal* I is such a subset of the ring that is closed under addition as well as under multiplication by a polynomial from $\mathbb{C}[x_1, x_2, \ldots, x_n]$. Specifically,

$$\forall f_1, f_2 \in I \ : \ f_1 + f_2 \in I$$
$$\forall f \in I, h \in \mathbb{C}[x_1, x_2, \ldots, x_n] \ : \ hf \in I.$$

We can generate a geometrical object from an ideal, as outlined in the next definition.

Definition 2.3.2. We define a function $\mathbf{V}(I) = V$, where $I \subset \mathbb{C}[x_1, x_2, \ldots, x_n]$, and $V \subset \mathbb{C}^n$.

$$\mathbf{V}(I) = \{a \in \mathbb{C}^n \mid f(a) = 0 \text{ for all } f \in I\}$$

Intuitively, V is a set of solutions to a (possibly infinite) system of polynomial equations I.

The geometrical sets that can be constructed as TP: in such a way are called varieties.

Definition 2.3.3. *A variety* V is such a set $V \subset \mathbb{C}^n$ that $\mathbf{V}(I) = V$ for some system of polynomial equations $I \subset \mathbb{C}[x_1, x_2, \ldots, x_n]$.

We can also generate an ideal back from a variety.

Definition 2.3.4. We define a function $\mathbf{I}(V) = I$, where $V \subset \mathbb{C}^n$, and $I \subset \mathbb{C}[x_1, x_2, \ldots, x_n]$.

$$\mathbf{I}(V) = \{f \in\subset \mathbb{C}[x_1, x_2, \ldots, x_n] \mid f(a) = 0 \text{ for all } a \in V\}.$$

Intuitively, I is a maximal set of polynomial equations that determines the geometrical set V.

A known result [5] is that $\mathbf{V}(\mathbf{I}(V)) = V$. Under a certain assumption[7], the opposite is also true $\mathbf{I}(\mathbf{V}(I)) = I$.

An important notion of Gröbner bases is somewhat analogical to linear bases from linear algebra.

Definition 2.3.5. *A Gröbner basis* $G = \{g_1, g_2, \ldots, g_m\} \subset I$ of an ideal $I \subset \mathbb{C}[x_1, x_2, \ldots, x_n]$ is such a set that

$$I = \langle g_1, g_2, \ldots, g_m \rangle = \{\sum_{i=1}^{m} h_i g_i \mid h_1, h_2, \ldots, h_m \in \mathbb{C}[x_1, x_2, \ldots, x_n]\}$$

An important result [5] states that every ideal defined on a finite-dimensional polynomial ring has a finite Gröbner basis. Continuing the analogy with linear bases, a Gröbner basis of a degree 1 polynomials (i.e., linear equations) system is indeed its linear basis.

TP: Written very well :-)

[7] When the ideal concerned is a so-called radical ideal [5].

3 Related work

Hartley and Silpa-Anan TP: delte: in the paper [9] develop an iterative algorithm which incorporates heuristic estimates (prior knowledge) of focal lengths. They also show that by allowing the algorithm to move principal point TP: , a better results can be achieved TP: obtained. The algorithm shows competitive, although not decisively better performance in comparison to 7pt approach. The authors also assume that an imaginary focal length cannot be used in any way for reconstruction, a supposition that we will show to be incorrect.

Nakatsuji et al. [14] show that even when the two focal lengths are known to be the same, the 7pt algorithm (which assumes they are different) yields better accuracy than methods which assume the same focal length. They also consider an imaginary focal length a failure and use 'subsampling' procedure to get a real one instead. Points are subsampled from the set of inliers and focal length is recomputed from the sample each time until a real focal length is found.

Kanazawa et al. [13] use 3 views for computing camera parameters (only two-view correspondences are needed for the method). Exploiting 3 TP: three different view pairs they are able to give more stable results than two-view methods.

DeepFocal, a recent algorithm by Scott Workman et al. [22] TP: , uses a Convolutional Neural Network to estimate the focal length directly from one image. The neural network outperforms other approaches based on one view. While an interesting and fresh idea, authors didn't compare DeepFocal to any existing two-view approaches, therefore it is difficult to assess Tthe advantages competitiveness of the work.

4 Experimental analysis of existing solutions

We assess the quality and stability of the 7pt algorithm with the Bougnoux formula. We consider this pipeline as essentially integral TP: baseline procedure for estimation of the focal lengthTP: s from image correspondences.

4.1 Experimental setup

We assume zero skew and unity aspect ratio in both cameras and consider a partially calibrated problem, i.e., the principal points are known. We assume that the images were translated TP: not clear what "translated" means in a way that principal points are always in the center. This means that the calibration matrices after this preprocessing are of shape

$$\mathtt{K}_i = \begin{bmatrix} f_i & 0 & 0 \\ 0 & f_i & 0 \\ 0 & 0 & 1 \end{bmatrix}.$$

The cameras are allowed to have different focal lengths.

4.1.1 Evaluation procedure

The setup for most experiments in the work is as follows:

Data: TP: The Number of correspondences used TP: is equal to n, level of noise σ TP: "level" is not precise enough". What is σ?

1 **begin**
2 Create a camera pair $\mathtt{P}_1$, $\mathtt{P}_2$ with focal lengths f_1,f_2;
3 Create a point cloud $\mathtt{X} \in \mathbb{R}^{3\times n}$ of n points in 3D ;
4 Project $\mathtt{X}$ to the cameras $\mathtt{P}_1$ and $\mathtt{P}_2$, producing the ground truth image point sets $\mathtt{x}_1^{gt}$, $\mathtt{x}_2^{gt} \in \mathbb{R}^{2\times n}$ TP: delete: correspondingly ;
5 Apply additive noise drawn from $\mathcal{N}(0, \sigma^2)$ to both x, y coordinates of each point from $\mathtt{x}_1^{gt}$ and $\mathtt{x}_2^{gt}$. This produces observed image point sets $\mathtt{x}_1^{ob}$ and $\mathtt{x}_2^{ob}$ correspondingly ;
6 Select 7 pairs of corresponding points $\mathtt{x}_1$ and $\mathtt{x}_2$, and let the remaining pairs to be the test set $\mathtt{x}_1^{test}, \mathtt{x}_2^{test}$;
7 Get the $\mathtt{F}_i$ estimates of the fundamental matrix $\mathtt{F}$ from the correspondences $\mathtt{x}_1, \mathtt{x}_2$ (e.g. $i = 1 \dots 3$ when using the 7pt algorithm 1). Leave only matrices with real elements;
8 Choose the estimation that optimizes Sampson error 4.1 on the test set;
9 Estimate the focal lengths from the fundamental matrix $\mathtt{F}$ (TP: why e.g. using the formulae 2.6 and 2.7);
10 **end**

Algorithm 3: Workflow

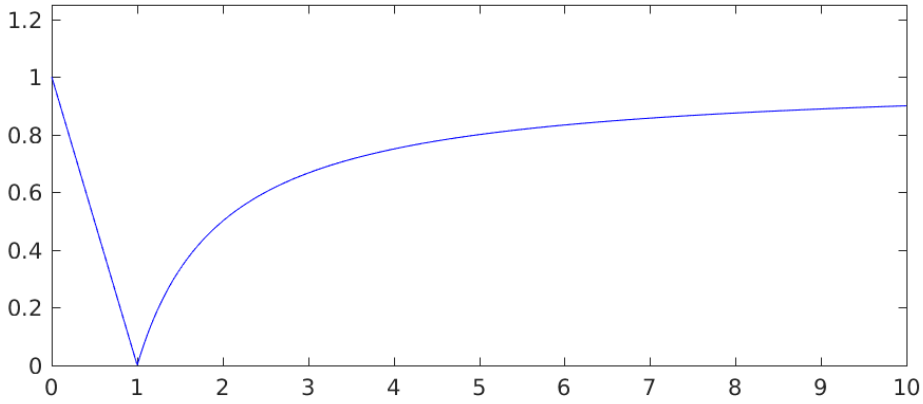

Figure 4.1 Error function for $f_{gt} = 1$

4.1.2 Estimation quality measure

We treat error in focal length estimation as multiplicative, so that the error in case where the ground truth $f_{gt} = 1000$ and computed value $f_{ob} = 2000$ is the same as error in case where the ground truth $f_{gt} = 100$ and computed value $f_{ob} = 200$. More precisely the error is given by

$$e(f_{gt}, f_{ob}) = 1 - \frac{\min(f_{gt}, f_{ob})}{\max(f_{gt}, f_{ob})}.$$

The error function for fixed ground truth value $f_{gt} = 1$ is shown at the figure 4.1.

For measuring TP: the quality of TP: a fundamental matrix we use the Sampson error:

$$S(\mathtt{F}) = \sum_i \frac{(\mathbf{x}_2^{\mathrm{T}}\mathtt{F}\mathbf{x}_1)^2}{(\mathtt{F}\mathbf{x}_1)_1^2 + (\mathtt{F}\mathbf{x}_1)_2^2 + (\mathbf{x}_2^{\mathrm{T}}\mathtt{F})_1^2 + (\mathbf{x}_2^{\mathrm{T}}\mathtt{F})_2^2} \tag{4.1}$$

4.2 Performance analysis for generic situations

In this section we suppose a generic scene, in which a degeneracy is unlikely to occur.

In experiments, we generate a random set of points and a random camera pairTP: s so that the set of correspondences in each image span at least 1000 × 1000 pixel square.

4.2.1 Overall analysis

We analyze the behavior of the pipeline against different numbers of given correspondences and different levels of noise. The quality of TP: the estimation is assessed by computing TP: the mean TP: of what? and two TP: which? quantiles of focal lengths computation error e. In these experiments we discard each TP: all imaginary estimateTP: s.

The graph 4.2 shows TP: a rapid decline in error with bigger TP: growing number of correspondences. Using 20 correspondences we can achieve an error close to negligible. This may be explained by the known fact that the 8pt solver optimizes error of matrix `F` in a certain sense TP: Explain better. What do you mean by "certain sense"? What do you mean by "error of matrix"?, as described by ? in [].

The graph 4.3 shows the growth of error with increasing noise. The number of used correspondences is 8 for both algorithms. We see that the error growth is approximately

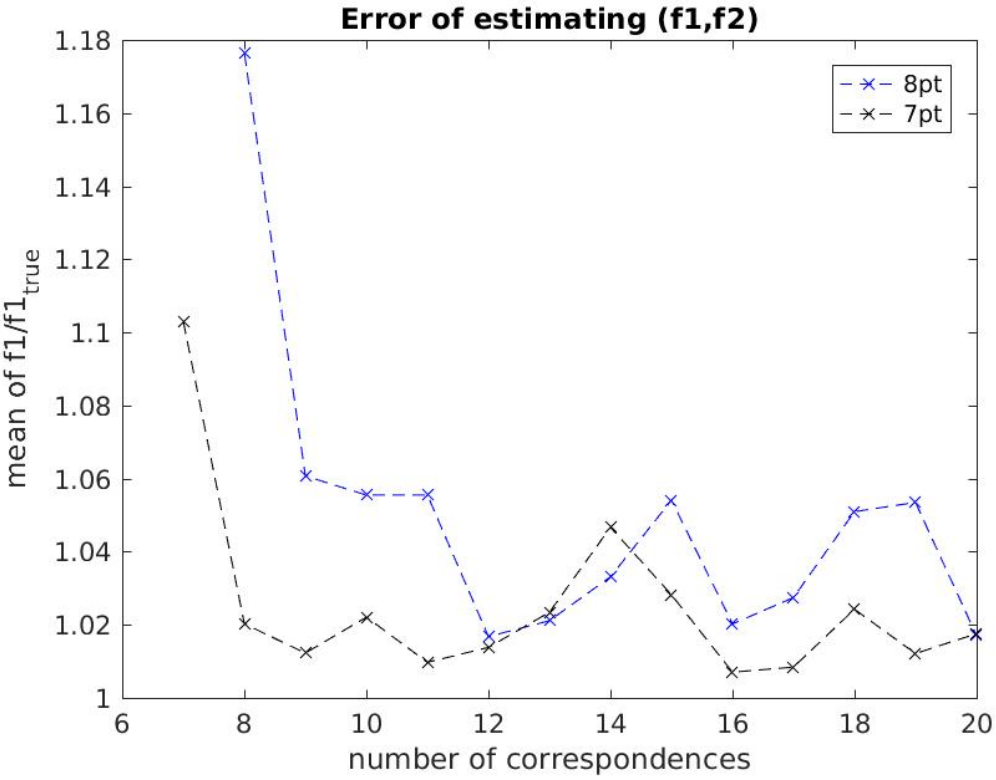

Figure 4.2 TP: A Comparison of TP: the 7pt and 8pt algorithms. Mean multiplicative error TP: Not celar what that is. Explain better. in focal length and two its quantiles TP: which are shown. TP: The Level of noise σ is TP: equal to 1. Imaginary estimates were excluded TP: delete: from experiment.

linear and quite mild, it can be seen that with additive noise of 3 pixels the error is still bearable. For realistic values of noise around 1 pixel, the error is reasonably small.

Another important trend showed on the graph 4.4 is the decrease of number of imaginary estimates with increasing number of used correspondences. We suggest that imaginary focal lengths are due to high level of noise, and appear less often when the noise is averaged over big number of correspondences.

We conclude that when the estimate of the focal lengths is real we can generally expect it to be quite precise and usable for most practical cases. More correspondences insure good performance, and moderate amounts of noise can be handled well. The 7pt algorithm performs better for most applications.

4.2.2 Ratio of focal lengths is robust

We empirically show that the ratio $r = f_2/f_1$ is more robust than f_1 or f_2.

To show it we conduct an experiment with a 300 different noise samples applied to the same camera geometry. The figure 4.5 shows scattered estimates of (f_1, f_2) vector. The method used for this experiment is 7pt with 7 correspondences. The noise level σ is 1. A few outliers were filtered out.

The graph shows scattered estimated points in the space (f_1, f_2). If this is space is not to have additional structure, we expect these estimations to lie on circles around the ground truth, perhaps similar to a 2 dimensional Gaussian distribution. However,

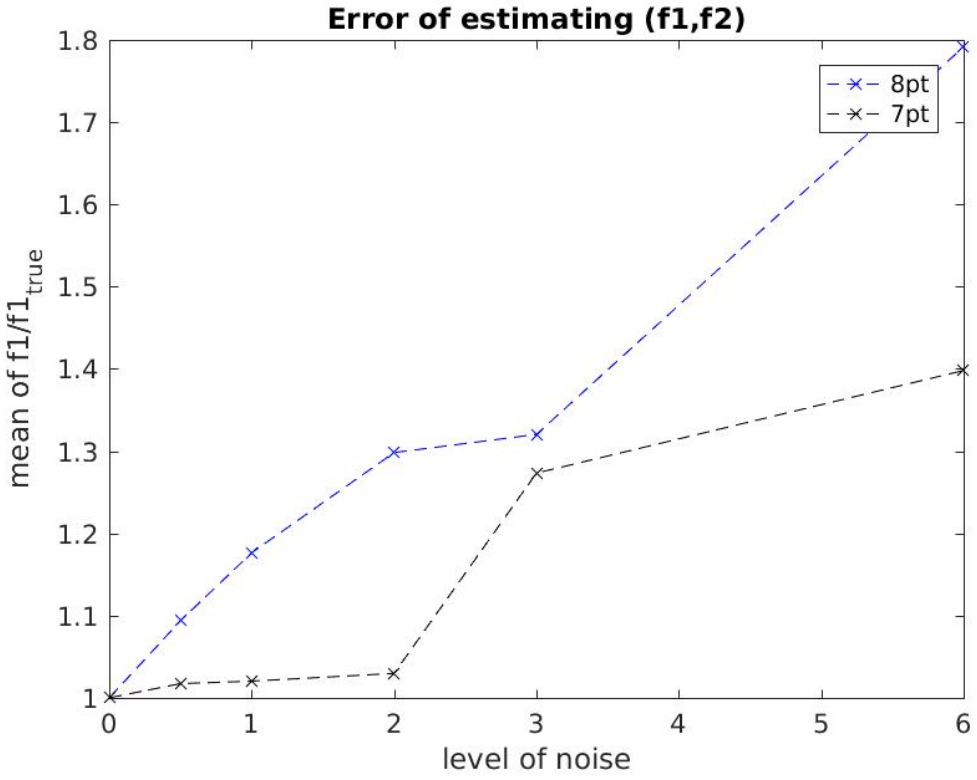

Figure 4.3 Comparison of 7pt and 8pt algorithms against noise level σ. 40 correspondences were used.

it can be seen that while the deviation of focal lengths is relatively big, the points clearly tend to the line $r = 3/4$ (given in blue), which is indeed the ground truth for the ratio. Imaginary estimates are also shown, and hint to a possibility that there is some structure to them also.

We conclude that ratio of the focal lengths r is more robust than the focal lengths themselves, which fact hopefully can be used later to construct a more robust solver.

4.2.3 Imaginary focal lengths

We empirically show that the ratio of the focal lengths is robust even when both focal lengths are imaginary. Our results also show that the probability of getting an imaginary focal length is not connected to distance between optical axes.

Figure 4.6 shows the experiment. The graph is a histogram of different errors in ratio (measured as $f_2/f_1 - (f_2/f_1)_{gt}$. The method used for this experiment is 7pt with 7 correspondences. The noise level σ is 1. A few outliers lie far off the graph.

Clearly, the likelihood that a focal lengths ratio is estimated better is bigger when the focal lengths are real. However, the graph shows that the ratios computed from imaginary focal lengths also fall reasonably close to ground truth, in the sense that mean of their distribution seemingly converges to ground truth. We suggest that there is a hidden variable that is susceptible to noise and makes both focal lengths imaginary when levels of noise are too high. It doesn't, however, affect ratio of focal lengths, or at least affects it to a lesser degree.

Figure 4.7 shows another experiment. One of our guesses was that the probability

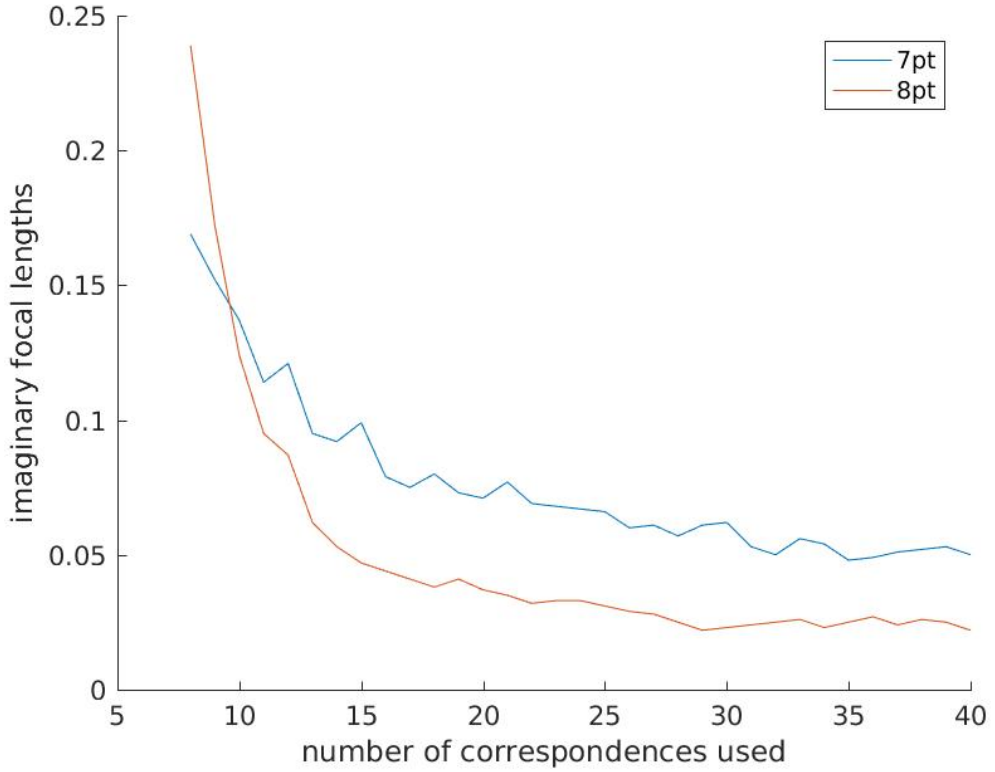

Figure 4.4 Fraction of imaginary focal length estimates produced by 7pt and 8pt algorithms. Noise level σ is 1.

of having imaginary estimate somehow correlates with closeness to degeneracy. In this experiment we assess the closeness by the optical axes transversal length. If the length is zero, optical axes intersect, and conversely, the bigger is transversal length, the further they are from intersecting.

We show the estimated ratios $r = f_2/f_1$. We see that even as transversal length increases, there is still approximately the same amount of imaginary estimates. We also see how both ratios computed from real and imaginary estimates tend to the ground truth line.

4.3 Performance analysis for close to degenerate situations

While in theory there does not exist a method to recover focal length when the optical axes intersect, with even small amount of noise the configuration no longer is singular. The focal length then can be computed in almost all practical situations. However, we expect a pose estimation method to deteriorate as the configuration becomes close to singular, due to numerical instability. Here we show the extent of this deterioration.

In this scenario, two optical axes are initially in a plane and we lift one camera away from the plane to distance d. The optical axes become skew lines as we move one of it away, and the distance between them is equal to d. We compare the quality of estimations for different distances d and levels of noise σ.

In our setup the distance between camera centers is 1 m and the mean distance from a camera to a point is 5 m. The algorithm used is 7pt and Bougnoux formula.

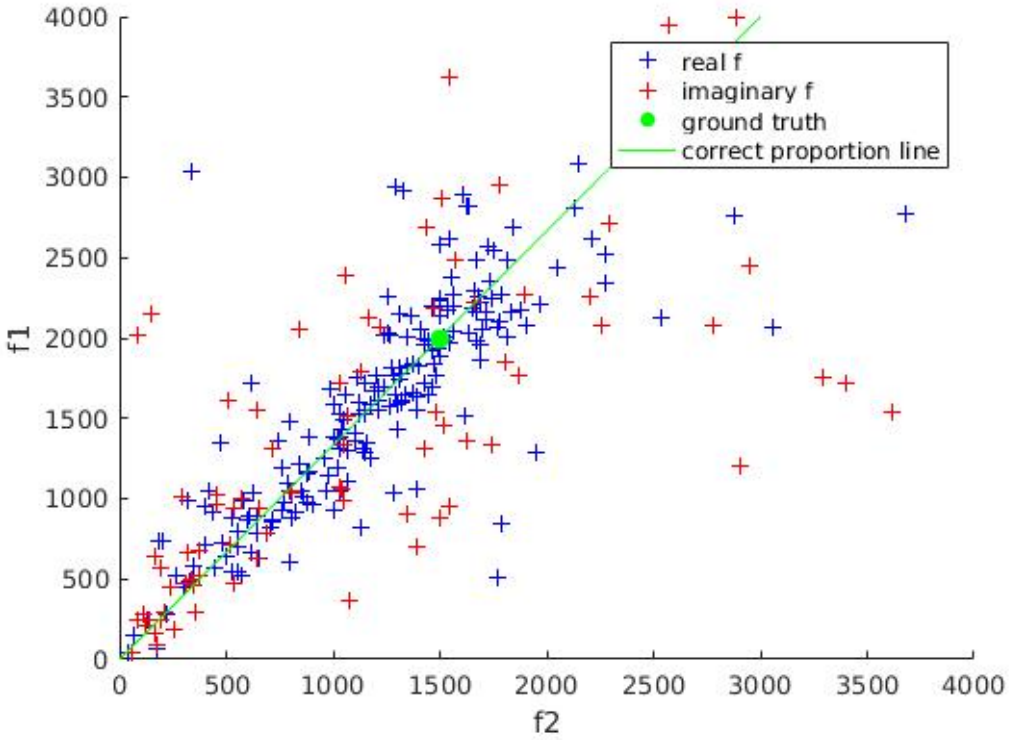

Figure 4.5 Scatter plot of 7pt focal lengths (f_1, f_2) estimates for one scene. Line through ground truth ratio $r = f_2/f_1$ is given for reference. Ground truth point also shown in green. Imaginary estimates shown in absolute value. Noise level σ is 1. 7 correspondences were used.

4.3.1 Intersecting optical axes

We empirically assess robustness of 7pt algorithm and Bougnoux formula in degenerate cases.

Figure 4.8 shows that for small values of noise, $\sigma \ll 0.1$px, distance between optical axes significantly affects 7pt method performance. The performance deteriorates greatly with decreasing distance. For more realistic noise levels, however, figure shows that the distance have little impact on quality of estimation. For 1 pixel noise the performance for intersecting axes and axes that have a 10 cm transversal is almost the same. A 50 cm transversal configuration, which we assume is not influenced by the degeneration is marginally more suitable for reconstruction. Even for configuration with axes distance zero, the performance is still acceptable (because of the noise presence), with 75% of estimations being off by a factor of at most 2.

We suggest this happens because the presence of noise drives the system further away from degenerate situation. The noise effect on camera geometry seemingly has a bias towards moving optical axes further from each other, which reduces the effect of numerical instability.

4.3.2 Parallel optical axes

A particular case of previous section configuration, is when the optical axes intersect at a point at infinity, i.e. are parallel.

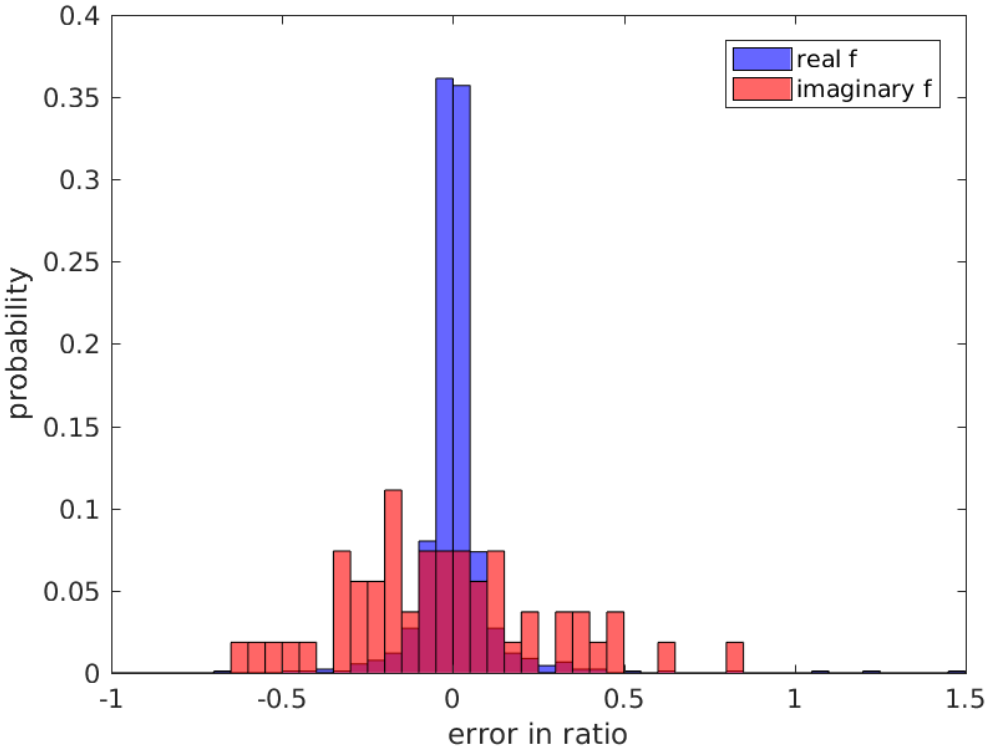

Figure 4.6 Distribution of errors in ratio $r - r_{true}$ produced by 7pt. Separate distributions are shown for the case with both real focal lengths and for the case with at least one imaginary. Red color is where an orange is supersimposed with blue. 40 correspondences were used, and level of noise σ is 1. Small number of outliers lie far off the graph.

In this scenario, two optical axes are initially parallel and we rotate one axis away from the common plane of the axes by an angle α. As we rotate one axis away, it is no longer parallel to the other one. We compare the quality of estimations for different distances d and levels of noise σ.

The figure 4.9 shows the results. We see that in this case, quality of estimation deteriorates even for significant amount of noise. At the elevation angle of 10° the degeneracy is no longer apparent, but for smaller angles performance visibly deteriorates.

4.3.3 Conclusions

We have seen that using more correspondences allow us to make much better results and get imaginary estimates less often. The ratio $r = f_2/f_1$ seems to be more robust than the focal lengths themselves. The ratio is also usable even when the focal lengths are imaginary.

Of two types of camera configuration degeneracy, intersecting optical axes do not pose a significant risk for camera reconstruction, especially for real-life noise levels. A configuration with parallel or nearly parallel optical axes, however, is a harder case where more than a half of reconstructions may be off by a factor of two and more.

f

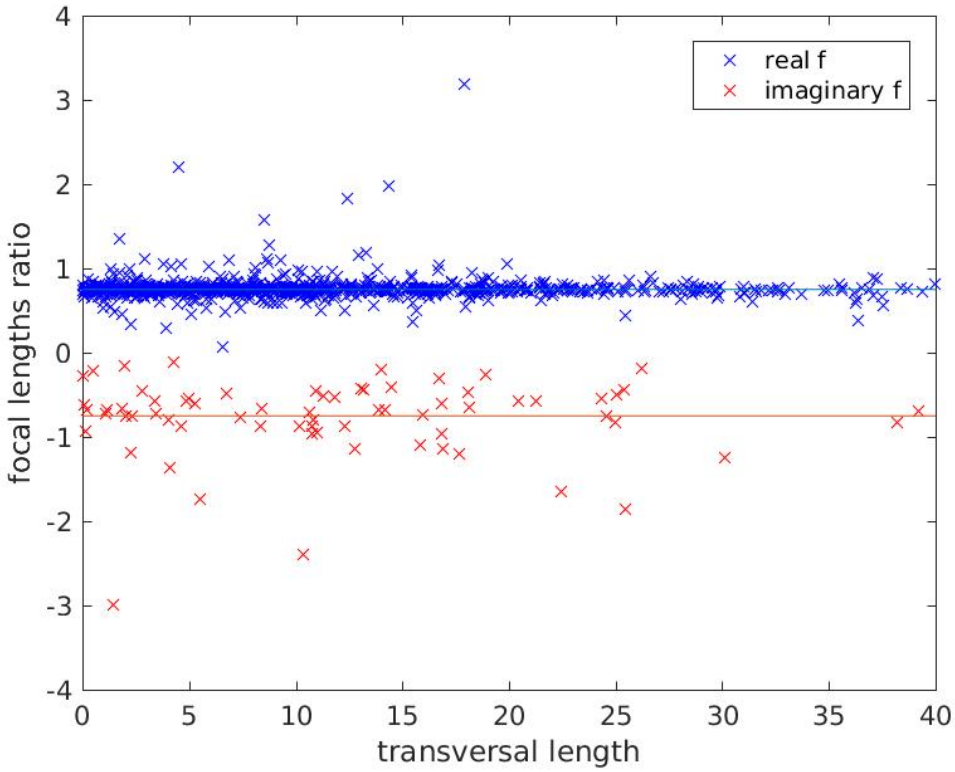

Figure 4.7 Scatter plot of focal lengths ratio $r = f_2/f_1$ estimates produced by 7pt. Ratios corresponding to imaginary focal lengths are plotted as negative to distingish them (they are positive). On X axis is the distance between optical axes. Small number of outliers lie far off the graph. 40 correspondences were used.

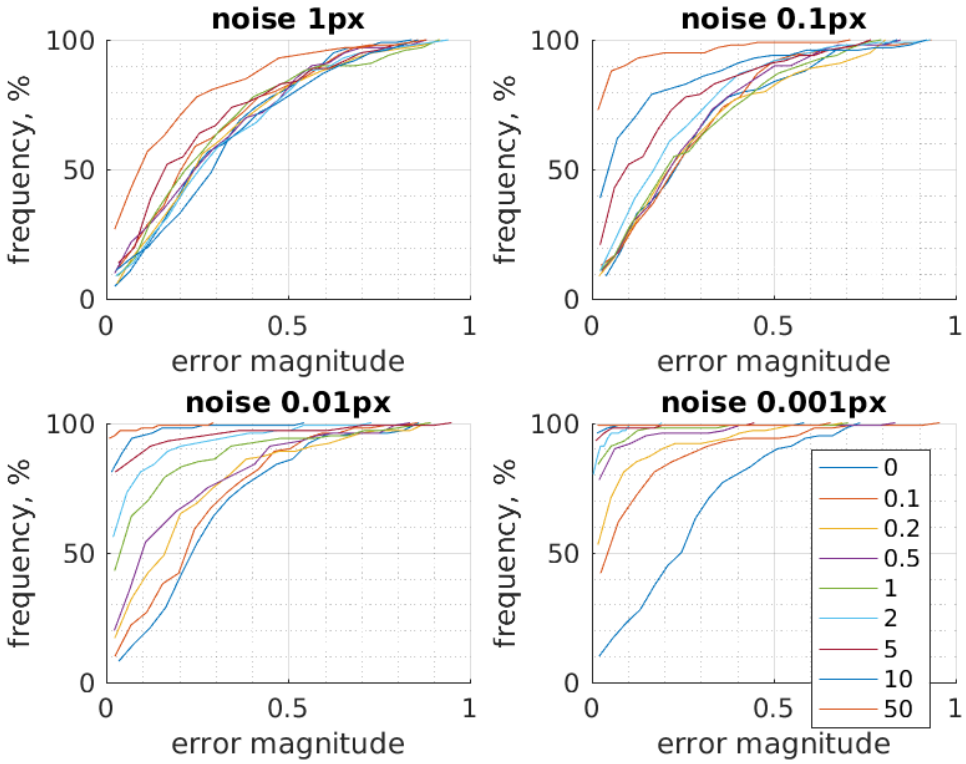

Figure 4.8 Cumulative distribution of estimated focal length multiplicative error for nearly intersecting optical axes. Different lines show different distances between optical axes in centimeters.

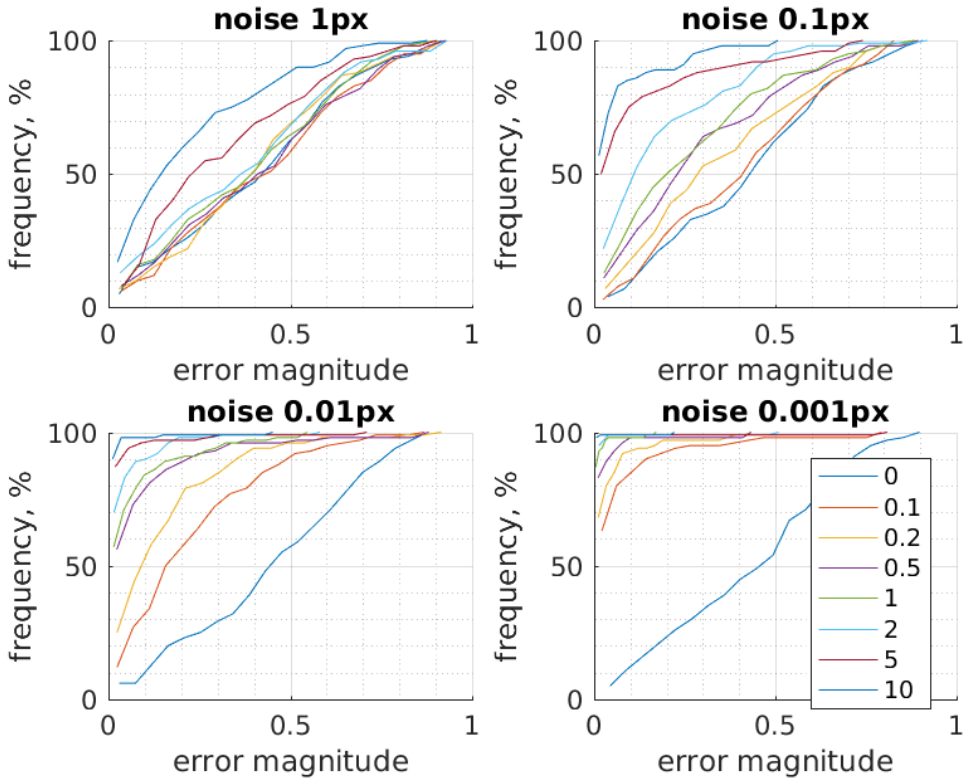

Figure 4.9 Cumulative distribution of estimated focal length multiplicative error for nearly parallel optical axes. Different lines show different angles between optical axes in degrees.

5 Set of fundamental matrices

In this section we analyze the 7pt algorithm from the algebraic geometry point of view. We show that indeed three and only three fundamental matrices (some possibly complex or of rank 1) can be derived using algebraic geometry. We analyse degeneracies and show that the only major degeneracy occurs when $\mathtt{F}_{3,3} = 0$. In this case the focal lengths are not determined, i.e. they may be anything from the interval $< -\infty, \infty >$. We also show that three different formulae exist for computing focal lengths from a Fundamental matrix (one being the Bougnoux formula).

5.1 Analysis

We analyse the set of valid fundamental matrices over complex numbers using techniques of algebraic geometry. To this end, we use Macaulay2 [7], a programming language and also a software pack for algebraic geometry and abstract commutative algebra. Macaulay2 tends to have an intuitive interface for many algebraic operations and in general code can be read as easily as mathematical equations. For this reason, instead of mathematical operations we will in this section use directly Macaulay2 code snippets. This also has the advantages of our results being easy reproducible.

In algebraic terms, we choose to describe the set of valid Fs as a variety in a complex numbers' field $\mathbb{C}^{11}$ of 11 variables, 9 for elements of the fundamental matrix F and 2 for focal lengths f_1, f_2.

The ideal Gs is the ideal generated by rank 2.5 and trace constraints 2.2 and saturated by the ideal $< f_1 * f_2 >$. The saturation is desirable, because the case when $f_1 = 0$ or $f_2 = 0$ doesn't correspond to any real camera system. Below is a snippet of Macaulay2 code explaining construction of Gs.

```
R = QQ[f1,f2,f11,f12,f13,f21,f22,f23,f31,f32,f33, MonomialOrder=>Lex]
F = matrix{{f11,f12,f13},{f21,f22,f23},{f31,f32,f33}}
K1 = matrix{{f1, 0, 0}, {0, f1, 0}, {0, 0, 1}}
K2 = matrix{{f2, 0, 0}, {0, f2, 0}, {0, 0, 1}}
E = transpose(K2)*F*K1 -- Essential matrix
G = ideal(det(E)) + minors(1, 2*E*transpose(E)*E - trace(E*transpose(E))*E);
dim G, codim G, degree G
Gs = saturate(G,ideal(f1*f2)); -- det(K1),det(K2) are non-zero
dim Gs, codim Gs, degree Gs
```

The ideal Gs contains conditions under which a matrix is generically a fundamental matrix. The variety $\mathbf{V}(Gs)$ therefore is a variety that contains all valid fundamental matrices. It also contains more matrices, specifically those of rank 0 and 1. Generically, however, we expect a matrix from the variety to be of rank 2. Moreover, the variety does contain some complex matrices. In practical situations however,, when considering a solver constructed this way, we can just sort out the spurious solutions afterwards as there will be only three solutions in total.

The 7pt algorithm can be regarded as intersecting the variety $\mathbf{V}(Gs)$ it with 7 hyperplanes, and it gives us three different solutions. Therefore we would expect the ideal

Gs to have dimension 7 and degree 3, but in reality, as constructed, it has dimension of 8 and degree of 58. This is explained by the fact that the variety $\mathbf{V}(Gs)$ has an additional component of dimension 8 and degree 58. Executing 7pt algorithm can be viewed as adding epipolar constraints to the ideal, and later we will see that this component doesn't survive the procedure.

The next snippet shows how to compute algebraic conditions in terms of elements of Fundamental matrix only, by eliminating f_1, f_2.

```
M = eliminate(Gs,{f1,f2});
dim M, codim M, degree M
-- the commands "mingens gb" give a minimal set of generators for the groebner basis of an
m = mingens gb M
```

After executing, we see that the ideal M has only one generator - the det(F) polynomial. This means that the constraints are the same as for the fully uncalibrated camera case [**?**]. It can be deduced that a seven-tuple of corresponding points obtained by fully uncalibrated cameras can also be explained by cameras with two unknown focal lengths when the focal lengths are allowed to attain non-real values.

It also means that only the singularity constraint **??** is needed to solve the system, and the Demazure constraints are extraneous.

5.2 Computing focal lengths

In the next snippet we also show how the Bougnoux formula [3] can be derived with algebraic geometry, given as a polynomial in the entries of F. This is done by eliminating one of the focal lengths from the ideal Gs. Turns out that the Gröbner basis of the eliminated ideal s_i contains 3 polynomials, and from each a formula for computing the focal length that wasn't eliminated can be deducted. This means that there exist three algebraically independent constraints on each focal length.

```
s2 = mingens gb eliminate(Gs,f1)
s1 = mingens gb eliminate(Gs,f2)
-- Formulae for f1
(m11,c11) = coefficients(s1_1_0,Variables=>{f1}) -- extract coefficients
(m12,c12) = coefficients(s1_2_0,Variables=>{f1}) -- extract coefficients
(m13,c13) = coefficients(s1_3_0,Variables=>{f1}) -- extract coefficients
-- Formulae for f2
(m21,c21) = coefficients(s2_1_0,Variables=>{f2}) -- extract coefficients
(m22,c22) = coefficients(s2_2_0,Variables=>{f2}) -- extract coefficients
(m23,c23) = coefficients(s2_3_0,Variables=>{f2}) -- extract coefficients
```

We see that there exist three formulae for each focal length, for example,

$$f_2^2 = -\frac{c23_{0,1}}{c23_{0,0}} =$$

$$= -\frac{f_{3,3}(f_{1,1}f_{2,3}f_{3,1} + f_{1,2}f_{2,3}f_{3,2} - f_{1,3}f_{2,1}f_{3,1} - f_{1,3}f_{2,2}f_{3,2})}{(f_{1,1}^2 f_{1,3}f_{2,3} - f_{1,1}f_{1,3}^2 f_{2,1} + f_{1,1}f_{2,1}f_{2,3}^2 + f_{1,2}^2 f_{1,3}f_{2,3} - f_{1,2}f_{1,3}^2 f_{2,2} + f_{1,2}f_{2,2}f_{2,3}^2 - f_{1,3}f_{2,1}^2 f_{2,3} - f_{1,3}f_{2,2}^2 f_{2,3})}.$$

It can be checked that this formula is equivalent to the Bougnoux formula by expressing the latter directly in terms of Fundamental matrix elements. The two more formulae are:

$$f_2^2 = -\frac{c21_{0,1}}{c21_{0,0}} = \tag{5.1}$$

$$= -\frac{f_{3,3}(f_{2,1}f_{3,1}f_{3,3} + f_{2,2}f_{3,2}f_{3,3} - f_{2,3}f_{3,1}^2 - f_{2,3}f_{3,2}^2)}{(f_{1,1}f_{1,3}f_{2,1}f_{3,3} - f_{1,1}f_{1,3}f_{2,3}f_{3,1} + f_{1,2}f_{1,3}f_{2,2}f_{3,3} - f_{1,2}f_{1,3}f_{2,3}f_{3,2} + f_{2,1}^2 f_{2,3}f_{3,3} - f_{2,1}f_{2,3}^2 f_{3,1} + f_{2,2}^2 f_{2,3}f_{3,3} - f_{2,2}f_{2,3}^2 f_{3,2})}. \tag{5.2}$$

$$f_2^2 = -\frac{c22_{0,1}}{c22_{0,0}} = \tag{5.3}$$

$$= -\frac{f_{3,3}(f_{1,1}f_{3,1}f_{3,3} + f_{1,2}f_{3,2}f_{3,3} - f_{1,3}f_{3,1}^2 - f_{1,3}f_{3,2}^2)}{(f_{1,1}^2 f_{1,3}f_{3,3} - f_{1,1}f_{1,3}^2 f_{3,1} + f_{1,1}f_{2,1}f_{2,3}f_{3,3} + f_{1,2}^2 f_{1,3}f_{3,3} - f_{1,2}f_{1,3}^2 f_{3,2} + f_{1,2}f_{2,2}f_{2,3}f_{3,3} - f_{1,3}f_{2,1}f_{2,3}f_{3,1} - f_{1,3}f_{2,2}f_{2,3}f_{3,2})}. \tag{5.4}$$

The formulae for another focal length may be obtained by transposing the fundamental matrix. The undertaken analysis of the formulae has shown that they differ very little in terms stability and quality of estimations.

Note that we reveal an additional degeneracy when each of the three denominators vanishes. This degeneracy was not previously known, and the focal lengths cannot be reconstructed from the matrix `F` when it occurs, as there are no constraints on them (they can have any value).

5.3 The ratio formula

We also present a formula to compute directly the ratio $r = f_2/f_1$.

$$r = \frac{(f_{1,1}^2 f_{3,1}^2 f_{3,3} + 2f_{1,1}f_{1,2}f_{3,1}f_{3,2}f_{3,3} - f_{1,1}f_{1,3}f_{3,1}^3 - f_{1,1}f_{1,3}f_{3,1}f_{3,2}^2 + f_{1,2}^2 f_{3,2}^2 f_{3,3} - f_{1,2}f_{1,3}f_{3,1}^2 f_{3,2} - f_{1,2}f_{1,3}f_{3,2}^3 + f_{2,1}^2 f_{3,1}^2 f_{3,3} + 2f_{2,1}f_{2,}}{(f_{1,1}^2 f_{1,3}^2 f_{3,3} - f_{1,1}f_{1,3}^3 f_{3,1} + 2f_{1,1}f_{1,3}f_{2,1}f_{2,3}f_{3,3} - f_{1,1}f_{1,3}f_{2,3}^2 f_{3,1} + f_{1,2}^2 f_{1,3}^2 f_{3,3} - f_{1,2}f_{1,3}^3 f_{3,2} + 2f_{1,2}f_{1,3}f_{2,2}f_{2,3}f_{3,3} - f_{1,2}f_{1,3}f_{2,3}^2 f_{3,2} -}$$

Computing the ratio directly from `F` can offer more speed and stability than computing it from the focal lengths. Indeed, we observed that for close to degenerate situations, the formula, if marginally, is a better estimator.

5.4 Computing Fundamental matrix

We show in detail how the 7pt solver work from the viewpoint of algebraic geometry.

We first simulate a random set of correspondences. Skipping this code for brevity, assume that the matrix `B` is a matrix from 7pt algorithm (1).

In the next snippet we show detailed analysis of the computation results. The variety $\mathbf{V}(GBs)$ is the variety of all possible focal lengths that explain the generated correspondences.

```
m = transpose matrix {{f11,f12,f13,f21,f22,f23,f31,f32,f33}}
rank B
eB = B*m
IB = minors(1,eB)
GBs = Gs + IB
gGBS=mingens gb GBs
dim GBs, codim GBs, degree GBs
pGBS = minimalPrimes GBs
```

Ideal IB contains the epipolar constraints. By adding the ideals Gs and IB we combine the constraints and obtain an ideal that corresponds to a variaty of solutions for our correspondences.

Variety $\mathbf{V}(GBs)$ can consist of either 6 or 14 components, one of dimension 2, and the rest of dimension 0. We will show the significance of this fact and what are these components corresponding to.

The ideal corresponding to the component of dimension 2 contains a polynomial $f_{3,3}$, i.e., it represents the degenerate situation when $f_{3,3}$ and the cameras' optical axes intersect (or are parallel) by lemma 2.2.1. The ideal also does not contain any polynomial in f_1 or f_2, so neither of focal lengths can be determined as there are no constraints on them. Because of this, the component has dimension 2 - its two degrees of freedom are f_1 and f_2.

Components of dimension 0 are point varieties (all variables are determined there). The first contains the polynomials f_1 and f_2, which means it corresponds to a degenerate case when $f_1 = 0, f_2 = 0$. Technically, such a fundamental matrix satisfies all constraints and is an example of matrix having rank less than two (see the discussion in section 2.2.4). This case could be avoided by using variables $w_1 = \frac{1}{f_1}, w_2 = \frac{1}{f_2}$.

12 (or 4) other components can be divided into 3 groups (or 1 group), which correspond to 3 different Fundamental matrices (a single matrix). Each group includes 4 point varieties in form $f_1 = \pm C_1, f_2 \pm C_2$ where C_1, C_2 are constants. The reason for this is that the focal length actually only enters the Bougnoux formula, as well as formulae we derived **??**, in second degree, so it is impossible to determine it's sign[1].

We see that each group correspond to one of the three fundamental matrices as returned by 7pt algorithm. Sometimes, however, two of them would be complex. In this case we will get only one group, as our code considers varieties over real numbers.

5.5 Conclusions

We have shown how Bougnoux formula and 7pt algorithm work in terms of algebraic geometry. We have derived 2 new formulae for computing focal lengths from fundamental matrix, and a formula for computing ratio $r = f_2/f_1$. We showed that Bougnoux formula is subject to additional degeneracy, which wasn't described before. We confirmed that three and only three fundamental matrices can explain 7 correspondences. We showed that the trace constraint is redundant while solving 7pt problem.

[1] Of course for any practical application the situation is unambiguous, as the positive sign should always be chosen

6 New algorithm

6.1 f-Ratio

We present a new algorithm, called f-Ratio, for robust focal lengths computing. The algorithm uses information that the ratio of focal lengths is more robust to achieve superior accuracy. We analyze the performance of the algorithm and give its use cases.

6.1.1 Algorithm

The idea of the algorithm is to use a new solver that would compute F from 6 correspondences given the ratio $r = f_2/f_1$. We create such a solver using automatic generator [15]. The solver uses Demazure [19] polynomials in terms of elements of the matrix F, f_1, and r.

Otherwise a solver assuming fixed focal length $f_1 = f_2$ could be used, for example that of Torii et el. [21], by first rescaling

$$v_r = \begin{bmatrix} r & 0 & 0 \\ 0 & r & 0 \\ 0 & 0 & 1 \end{bmatrix} v.$$

The output of such solver would be f_1.

In both cases, the solver yield 15 (possibly non-real) solutions.

Data: list of 7 right image points u, list of the corresponding left image points v, lists of remaining tentative correspondences u_{test}, v_{test}, 6pt solver $solve6pt$
Result: Fundamental matrix F

begin
  From all correspondences estimate F_0 ;
  Estimate $ratio = f_2/f_1$ from F_0 ;
  foreach *6-tuple* u_6 *of points drawn from* u **do**
    $v_6 \leftarrow$ corresponding points to u_6 from v ;
    $Fs_i \leftarrow solve6pt(u_6, v_6, ratio)$;
    $F_i \leftarrow$ the matrix $\in Fs_i$ which best explains u_{test}, v_{test}.
  end
  return *the* F_i *which best explains* u_{test}, v_{test}.
end

Algorithm 4: f-Ratio

6.1.2 Performance

We assess the performance of the algorithm in a similar manner to previous analysis. In this experiment, we compare our method f-Ratio to baseline 7pt method.

We also plot the best reconstruction which was found by the procedure 4. In most cases the matrix chosen by the consensus set is not the best one available, which is reflected by this graph. We measure the "fitness" of the matrix in terms of focal lengths only in this case.

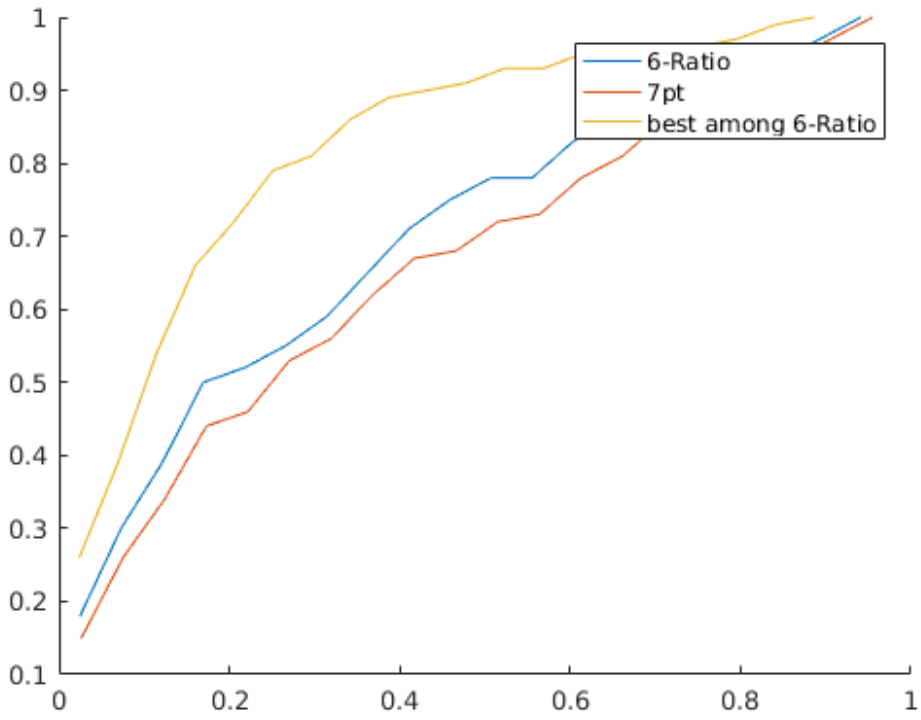

Figure 6.1 Error cumulative distribution showing performance of f-Ratio

In the next experiment, we add an amount of noise ($\sigma = 1$ pixels) to one of the points. This demonstrates that our method can cope with outliers even better than the standart RANSAC algorithm.

The results show that it is possible to reconstruct better scenes with our algorithm than with state-of-the-art 7pt algorithm. The big drawback is the speed of the algorithm. Since we need to test at most 7×15 matrices, our algorithm as given is an order of magnitude slower. In future work, this issue can be alleviated by analyzing the structure of matrices tested. Preliminary results has shown that there may be some repetitions.

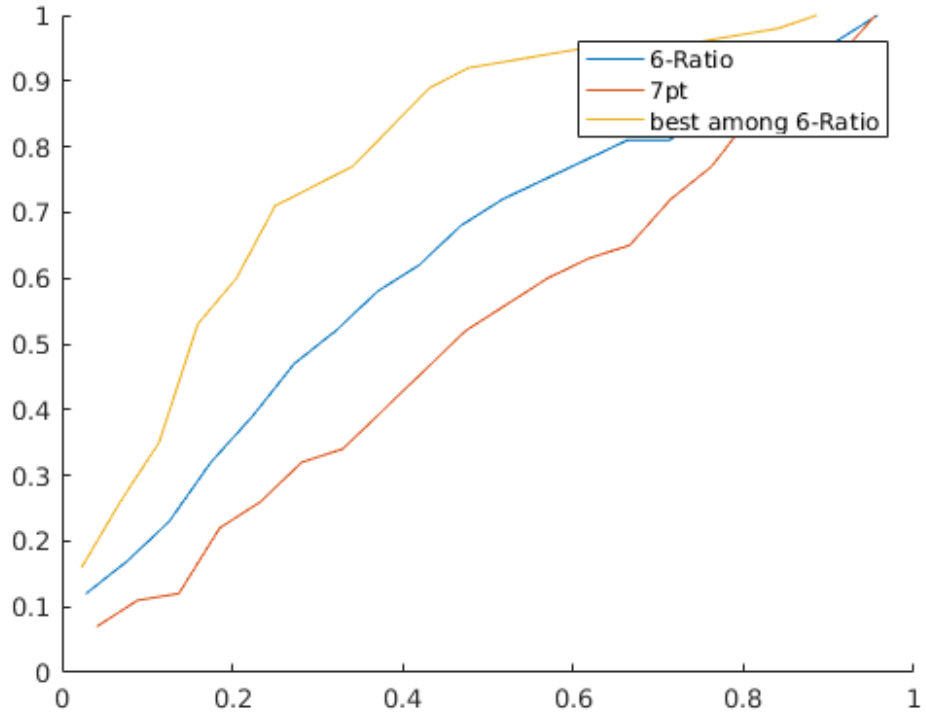

Figure 6.2 Error cumulative distribution showing performance of f-Ratio with one outlier

Bibliography

[1] Sameer Agarwal, Hon-leung Lee, Bernd Sturmfels, and Rekha R. Thomas. On the existence of epipolar matrices. *CoRR*, abs/1510.01401, 2015.

[2] Herbert Bay, Andreas Ess, Tinne Tuytelaars, and Luc Van Gool. Speeded-up robust features (surf). *Comput. Vis. Image Underst.*, 110(3):346–359, June 2008.

[3] Sylvain Bougnoux. From projective to euclidean space under any practical situation, a criticism of self-calibration. In *ICCV*, pages 790–798, 1998.

[4] David A. Cox, John Little, and Donal O'Shea. *Using Algebraic Geometry*. Springer-Verlag New York, Inc., Secaucus, NJ, USA, 2005.

[5] David A. Cox, John Little, and Donal O'Shea. *Ideals, Varieties, and Algorithms: An Introduction to Computational Algebraic Geometry and Commutative Algebra, 3/e (Undergraduate Texts in Mathematics)*. Springer-Verlag New York, Inc., Secaucus, NJ, USA, 2007.

[6] Martin A. Fischler and Robert C. Bolles. Random sample consensus: A paradigm for model fitting with applications to image analysis and automated cartography. *Commun. ACM*, 24(6):381–395, June 1981.

[7] Daniel R. Grayson and Michael E. Stillman. Macaulay2, a software system for research in algebraic geometry. Available at http://www.math.uiuc.edu/Macaulay2/.

[8] R. I. Hartley and A. Zisserman. *Multiple View Geometry in Computer Vision*. Cambridge University Press, ISBN: 0521540518, second edition, 2004.

[9] Richard Hartley and Chanop Silpa-anan. Reconstruction from two views using approximate calibration. In *Proc. 5th Asian Conf. Comput. Vision*, pages 338–343, 2002.

[10] Richard I. Hartley. In defense of the eight-point algorithm. *IEEE Trans. Pattern Anal. Mach. Intell.*, 19(6):580–593, June 1997.

[11] Richard I. Hartley. Chirality. *International Journal of Computer Vision*, 26(1):41–61, 1998.

[12] Kenichi Kanatani and Chikara Matsunaga. Closed-form expression for focal lengths from the fundamental matrix. In *in Proc. 4th Asian Conf. Computer Vision*, pages 128–133, 2000.

[13] Kenichi Kanatani, Atsutada Nakatsuji, and Yasuyuki Sugaya. Stabilizing the focal length computation for 3-d reconstruction from two uncalibrated views. *International Journal of Computer Vision*, 66(2):109–122, 2006.

[14] Yasushi Kanazawa, Yasuyuki Sugaya, and Kenichi Kanatani. Decomposing three fundamental matrices for initializing 3-d reconstruction from three views. *IPSJ Transactions on Computer Vision and Applications*, 6:120–131, 2014.

[15] Zuzana Kukelova, Martin Bujnak, and Tomas Pajdla. Automatic generator of minimal problem solvers. In *Computer Vision - ECCV 2008, 10th European Conference on Computer Vision, Proceedings, Part III*, pages 302–315, 2008.

[16] Zuzana Kukelova, Martin Bujnak, and Tomas Pajdla. Polynomial eigenvalue solutions to minimal problems in computer vision. *IEEE Transactions on Pattern Analysis and Machine Intelligence*, 34:1381–1393, 2011.

[17] H. C. Longuet-Higgins. Readings in computer vision: Issues, problems, principles, and paradigms. chapter A Computer Algorithm for Reconstructing a Scene from Two Projections, pages 61–62. Morgan Kaufmann Publishers Inc., San Francisco, CA, USA, 1987.

[18] David G. Lowe. Distinctive image features from scale-invariant keypoints. *Int. J. Comput. Vision*, 60(2):91–110, November 2004.

[19] Demazure M. Sur deux problemes de reconstruction. Technical Report 882, INRIA, 1988.

[20] Henrik Stewénius, David Nistér, Fredrik Kahl, and Frederik Schaffalitzky. A minimal solution for relative pose with unknown focal length. In *CVPR (2)*, pages 789–794. IEEE Computer Society, 2005.

[21] Akihiko Torii, Zuzana Kukelova, Martin Bujnak, and Tomás Pajdla. In *ACCV Workshops (2)*, 2010.

[22] S. Workman, C. Greenwell, M. Zhai, R. Baltenberger, and N. Jacobs. Deepfocal: A method for direct focal length estimation. In *2015 IEEE International Conference on Image Processing (ICIP)*, pages 1369–1373, Sept 2015.